ELSEVIER

Contents lists available at ScienceDirect

# Solid State Sciences

journal homepage: www.elsevier.com/locate/ssscie





# Targeting Oxide Concentration in Tantalum Oxide-Fluoride Anions

Kendall R. Kamp, Yiran Wang, Kenneth R. Poeppelmeier

Department of Chemistry, Northwestern University, 2145 Sheridan Road, Evanston, IL, 60208, USA

ABSTRACT

The design of both molecular and non-molecular solid materials with specific properties fundamentally relies on the controlled synthesis of crystals with desired functional groups, bonding motifs, polarity, chirality, and more. To this end, fluoride and oxide-fluoride anions have been utilized as basic building units (BBUs) in the synthesis of noncentrosymmetric racemic materials for their ability to create polar axes that facilitate the breaking of an inversion center as demonstrated in a series of compounds with  $[MF_6]^2$  anions (M = Ti, Zr, Hf). Targeting an analog with a  $[TaOF_5]^2$  anion, the phase space of  $(CuO, Ta_2O_5)/bpy/HF_{(aq)}/H_2O$  (bpy = 2,2′-bipyridine) was investigated and three new compounds with Cu-bpy cations and Ta-fluoride or Ta-oxyfluoride anions were synthesized:  $[Cu(bpy)_2][TaF_6]$ ,  $[Cu(bpy)_2][Ta_2OF_{10}]$ , and  $[Cu(bpy)F(H_2O)_2]_2[TaF_7]$ • $H_2O$  with the anions  $[TaF_6]^7$ ,  $[Ta_2OF_{10}]^2$ , and  $[TaF_7]^{2^7}$ , respectively. The formation of these anions was found to be a product of both the concentration of hydrofluoric acid in solution and the ratio of metal-oxide starting materials to ligand. This work contributes to the understanding of mixed anion formation in the solid state.

#### 1. Introduction

Many properties require certain symmetry elements to be present or absent, such as nonlinear optical activity and circular dichroism require the absence of an inversion center [1-4], while other properties require specific electronic [5,6], polarity, or geometric considerations [7]; examples include the electron counting rules in band theory to determine if the material is an insulator or conductor [8], a net polar moment for pyroelectricity [9,10], and triangular motifs to promote magnetic frustration in some magnetic materials, respectively [11,12]. It is therefore a foundation to designing molecular and non-molecular solid materials with specific properties to know what synthetic conditions yield desired structural functional groups, building units, bonding motifs and the like. To this end, using basic building units (BBUs) with mixed anions to assemble materials is a promising route to materials design [13]. Further, combining different BBUs with different symmetry or polarity elements allows for an additive approach to materials design: such has been seen through the combination of chiral and polar BBUs in the synthesis of noncentrosymmetric racemate compounds [1,14,15].

Tantalum anions host a wide variety of sizes, geometries, and polarities, making them candidate BBUs for a wide variety of materials with physical properties [16–19]. Further, the solubility of tantalum oxide ( $\text{Ta}_2\text{O}_5$ ) in hydrofluoric acid solutions allows for extensive study of Ta-fluoride and Ta-oxide/fluoride anions [2,13,18–20]. Ta-fluoride anions [ $\text{TaF}_x$ ]<sup>5-x</sup> range from octahedral (x=6) to the distorted capped-cube of (x=9) and the octahedral dimer [ $\text{Ta}_2\text{F}_{11}$ ] [21–25].

Ta-oxyfluoride anions exhibit an even broader range of sizes and geometries, from octahedral  $[TaOF_5]^{2-}$  to its dimer  $[Ta_2OF_{10}]^{2-}$  [26], and tetramer  $[Ta_4O_4F_{16}]^{4-}$  [19], adamantane-like cage  $[Ta_4O_6F_{12}]^{4-}$  [27], the hexanuclear cage-like cluster  $[Ta_6O_9F_{18}]^{3-}$  [19], and one dimensional chains of  $[TaOF_4]$  and more [19,28-30]. Further, the formation of many of these fluoride and oxyfluoride anions is understood through the relationship of the amount of dissociation of aqueous hydrofluoric acid and organic bases needing protonation, therefore, controlling the amount of fluoride ions in solution [18,19].

In this article, we report three new Ta-fluoride and Ta-oxyfluoride compounds. Chiral, metal-centered BBUs were combined with Ta-fluoride/oxyfluoride anions targeting a noncentrosymmetric, polar, racemate with the anion  $[TaOF_5]^2$ , a Group V, oxyfluoride analog to the Group IV series of compounds of the formula  $\Delta$ ,  $\Lambda$ -[Cu(bpy)<sub>2</sub>.  $H_2O]_2[MF_6]_2 \bullet H_2O$  (bpy = 2,2'-bipyridine, M = Ti, Zr, or Hf) [14,15]. Exploratory synthesis towards this target yielded the compounds [Cu (bpy)<sub>2</sub>][TaF<sub>6</sub>] (1), [Cu(bpy)<sub>2</sub>][Ta<sub>2</sub>OF<sub>10</sub>] (2), and [Cu(bpy)F ( $H_2O$ )<sub>2</sub>]<sub>2</sub>[TaF<sub>7</sub>] $\bullet$ H<sub>2</sub>O (3) with the anions [TaF<sub>6</sub>], [Ta<sub>2</sub>OF<sub>10</sub>]<sup>2</sup>, and [TaF<sub>7</sub>]<sup>2</sup>, respectively. These newly synthesized compounds are structurally characterized and the formation of the anions in the presence of metal chelated cations builds on the works by Lu [18] and Wu [19] which described the basicity of organic bases and anion formation, as well as the role of acid concentration in conjunction with the basic ligands.

E-mail address: krp@northwestern.edu (K.R. Poeppelmeier).

Abbreviations: BBU, basic building unit; bpy, 2-2'-bipyridine; ETM, early transition metal.

<sup>\*</sup> Corresponding author.

#### 2. Methods

Hydrofluoric acid (HF) is toxic and corrosive! HF must be handled with extreme caution and with the appropriate protective gear [31–33].

#### 2.1. Materials

 $Ta_2O_5$  (Aldrich, 99 % trace metals basis), CuO (Sigma-Aldrich,  $\geq$ 99.0 %), 2,2'-bipyridine (bpy, Sigma-Aldrich,  $\geq$ 99 %), HF $_{(aq)}$  (Sigma-Aldrich, 48 % wt. in H $_2$ O,  $\geq$ 99.99+% trace metals basis) were used as received. Reagent amounts of deionized water were used.

# 2.2. Hydrothermal Synthesis

The compounds reported in this article were synthesized via the hydrothermal pouch method [15]. In each reaction, heat sealed Teflon pouches were charged with reagents and loaded into a 125 mL Parr autoclave in sets of six with 40 mL deionized water added as backfill. Autoclaves were heated at a rate of 5 °C/min to 200 °C (compound 1) or 150 °C (compounds 2 and 3) and held for 24 h before slow cooling at a rate of 0.1 °C/min to room temperature. Solid products were recovered by vacuum filtration.

Compound 1,  $[Cu(bpy)_2][TaF_6]$  was synthesized in a pouch containing 0.1707 mmol CuO, 0.0854 mmol  $Ta_2O_5$ , 0.2538 mmol bpy, 0.4 mL  $HF_{(aq)}$  (11.04 mmol), and 0.7 mL deionized water. Orange block crystals were recovered by vacuum filtration along with the phase [Cu  $(bpy)_3$ ][ $TaF_6$ ]<sub>2</sub> [34].

Compound **2**,  $[Cu(bpy)_2][Ta_2OF_{10}]$  was synthesized in a pouch containing 0.0415 mmol CuO, 0.0829 mmol  $Ta_2O_5$ , 0.2070 mmol bpy, 0.4 mL  $HF_{(aq)}$  (11.04 mmol), and 0.15 mL deionized water. Blue plate crystals were recovered by vacuum filtration along with other unidentified phases.

Compound 3,  $[Cu(bpy)F(H_2O)_2]_2[TaF_7] \bullet H_2O$  was synthesized in a pouch containing 0.1707 mmol CuO, 0.0854 mmol  $Ta_2O_5$ , 0.2538 mmol bpy, 0.1 mL  $HF_{(aq)}$  (2.76 mmol), and 1 mL deionized water. Blue block crystals were recovered by vacuum filtration along with other unidentified phases.

# 2.3. Single Crystal X-ray Diffraction

Suitable single crystals were mounted on a MitiGen mount with paratone oil. The crystals were analyzed on a XtaLAB Synergy diffractometer equipped with a micro-focus sealed X-ray tube PhotonJet (MoK $\alpha$ ,  $\lambda=0.71073$  Å) source and a Hybrid Pixel Array (HyPix) detector at 100 K. Temperature was controlled by with an Oxford Cryostystems low-temperature device. Run list generation, data integration and finalization were performed with the CrysAlisPro software; [35] a numerical absorption correction was applied. The structure was solved using Intrinsic Phase matching as implemented in ShelXT [36] within the Olex2 program [37]. The crystallographic models were refined with ShelXT using a least squares minimization.

# 2.4. Diffuse Reflectance UV-Visible Spectrometry

The UV-VIS-NIR spectrum in diffuse reflectance mode was collected on lightly grounded powder using a Cary 5000 UV-Vis-NIR double beam spectrophotometer with a monochromator. BaSO<sub>4</sub> powder was used for the baseline collection, whereas a mixture of sample powder with BaSO<sub>4</sub> was used for the data collection at room temperature. Absorbance data was converted from reflectance data in-software using the Kubelka-Munk equation  $\alpha/S=(1\text{-R})^2/2R$ , where  $\alpha$  and S are the absorption and scattering coefficients respectively, and R is the reflectance.

#### 3. Results and Discussion

#### 3.1. Structural Descriptions

The formation conditions of different Ta-fluoride and Ta-oxyfluoride building units were investigated through their combination with Cu-bpy chiral units. Exploration of the CuO/Ta<sub>2</sub>O<sub>5</sub>/bpy/HF( $_{aq}$ ) system (bpy = 2,2′-bipyridine) yielded three new centrosymmetric compounds with three different Ta-oxyfluoride anions: TaF $_{0}^{-}$  (compound 1), Ta $_{2}$ OF $_{10}^{-}$  (compound 2), and TaF $_{2}^{-}$  (compound 3). An overview of the crystal structures of these compounds is given in Table 1.

Compound 1 has the formula  $[Cu(bpy)_2][TaF_6]$  and crystallizes in the triclinic space group P  $\overline{1}$ . The asymmetric unit is composed of one  $[Cu(bpy)_2]^+$  cation and one  $[TaF_6]^-$  anion. The cation displays  $C_1$  symmetry and has both handedness ( $\Delta$  and  $\Lambda$ ), with the enantiomers being related by an inversion center. The  $Cu^{2+}$  compound  $[Cu(bpy)_3][TaF_6]_2$  was also found in all samples containing compound 1, the tri-bpy complex has been characterized by Nisbet et al. [34]

To further investigate the geometry of the cations, the  $\tau_4$  parameter ( $\tau_4 = \frac{360 - (\alpha + \beta)}{360 - 2\theta}$ ,  $\theta = \cos^{-1}(\frac{1}{3}){\approx}109.5^{\circ}$ ) [38] was used, were  $\alpha$  and  $\beta$  are the two largest angles of the coordination center. The  $\tau_4$  parameter is an indicator of molecular geometry, with a value of 0 indicating a square planar geometry and a value of 1 corresponds to a tetrahedral geometry. In compound 1, the  $\tau_4$  value is 0.665 suggesting a distorted geometry that is neither square planar or tetrahedral.

Heterochiral  $\pi$ - $\pi$  stacking interactions between cation enantiomers of different handedness run along both the  ${\bf c}$  (Fig. 1a) and  ${\bf b}$  (Fig. 1b) axes. Torsion angles  $T_1$  and  $T_2$  were used to describe these interactions further, with the  $T_1$  angle representing the relative direction of the interacting ligands and the  $T_2$  angle defining the stacking interactions of the ligands (additional information on these angles can be found in the Supporting Information) [39,40]. For the heterochiral overlap along the  ${\bf b}$  axis,  $T_1$  is equal to 122.812° indicating the cations are arranged in a head-to-tail orientation; the  $T_2$  angle is equal to 86.887° signifying a nonparallel stacking interaction with one of the two  $C_5N$  rings overlapping. The same types of overlap are observed in heterochiral  $\pi$ - $\pi$  stacking interactions along the  ${\bf c}$  axis, where head-to-tail interactions with one overlapping  $C_5N$  ring overlap were observed ( $T_1 = 113.733^\circ$ ,  $T_2 = 48.827^\circ$ ) (see Figure 1).

The [TaF<sub>6</sub>] anion features six Ta–F bonds with lengths ranging from 1.8874 to 1.9005 Å: the variance in Ta–F bond lengths hints at a small out of center distortion creating a polar axis within the anion. The inversion center relating the two anions leads to a net cancellation of the anions' polar moments.

Compound **2** has the formula  $[Cu(bpy)_2][Ta_2OF_{10}]$  and crystallizes in the space group P  $\overline{I}$  and its asymmetric unit contains one cation and one anion. The full structure contains two of each, with cation and anion

**Table 1**Basic crystallographic information for compounds 1, 2, and 3. Complete crystallographic information is available in the Supporting Information.

	1	2	3
Formula	[Cu(bpy) <sub>2</sub> ]	[Cu(bpy) <sub>2</sub> ]	[Cu(bpy)F(H <sub>2</sub> O) <sub>2</sub> ] <sub>2</sub> [TaF7]•
	[TaF <sub>6</sub> ]	[Ta <sub>2</sub> OF <sub>10</sub> ]	$H_20$
Anion	TaF <sub>6</sub>	$Ta_2OF_{10}^{2-}$	TaF <sub>7</sub> <sup>2-</sup>
Space	$P\overline{1}(2)$	$P\overline{1}(2)$	$P2_1/c$ (14)
Group			
a (Å)	8.6142(2)	9.9747(2)	21.5414(2)
b (Å)	9.4665(2)	10.1496(2)	7.44480(10)
c (Å)	14.3714(2)	13.4325(3)	33.4908(2)
α (°)	107.742(2)	73.894(2)	90
β (°)	92.637(2)	74.678(2)	99.3450(10)
γ (°)	107.465(2)	70.793(2)	90
V (Å <sup>3</sup> )	1052.48(4)	1211.16(5)	5299.69(9)
Z	2	2	8
CCDC	2293940	2293941	2293943

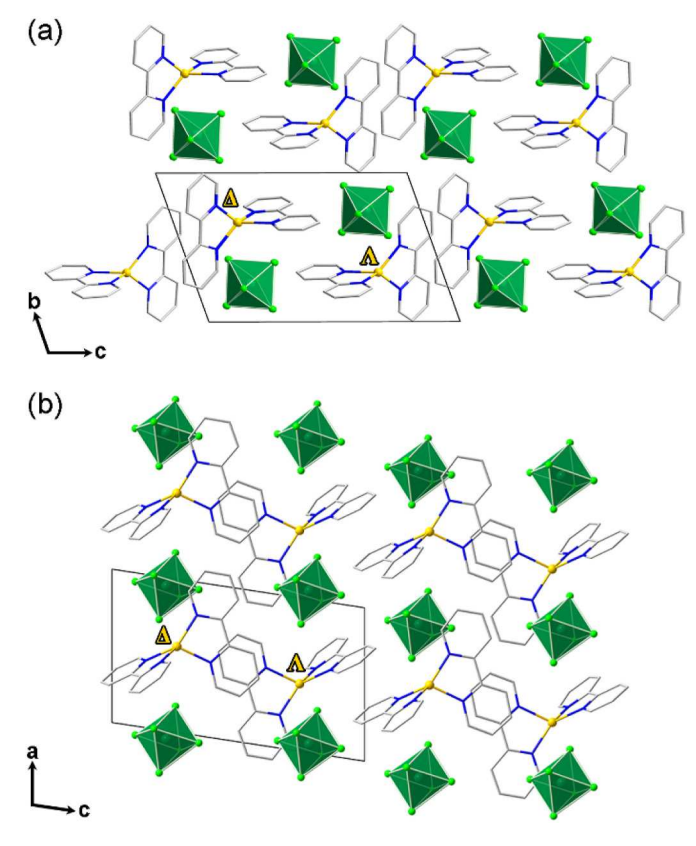


Fig. 1. Structure of Compound 1 as viewed down the (a)  $\bf a$  axis, and the (b)  $\bf b$  axis. Dark green, yellow, light green, blue, and gray spheres represent Ta, Cu, F, N, and C respectively, green polyhedra represent Ta-centered anions. Hydrogen atoms on the ligands have been omitted for clarity.

pairs related by an inversion center. The cation,  $\text{Cu}(\text{bpy})_2^{2^+}$  has  $C_1$  symmetry and displays both  $\Delta$  and  $\Lambda$  enantiomers stacking along the  $\mathbf{c}$  axis. With a  $\tau_4$  parameter value of 0.326, the geometry is between square planar and a tetrahedra. Torsion angles of 127.383° and 88.638° for  $T_1$  and  $T_2$  respectively, indicate a head-to-tail orientation of the heterochiral cations with nonparallel stacking and overlap of only one  $C_5N$  ring between (Figure 2).

The anion  $Ta_2OF_{10}^{2-}$  is a dimer of  $TaOF_5^{2-}$  anions corner sharing through the O atom. The dimer is not entirely linear with a Ta1-O-Ta2 angle of  $168.564^\circ$ ; further, out of center distortions occur within the Tacentered octahedra as the Ta-O bonds range from 1.9026 (Ta1-O) to 1.9111 Å (Ta2-O) and the Ta-F bonds range from 1.8962 to 1.9268 Å. It should be noted that the dimer anion observed differs from previous literature reports for its non-linear connection of the dimer as well as its longer Ta-O/F bond lengths [26,41,42].

Compound **3** has the formula  $[Cu(bpy)F(H_2O)_2]_2[TaF_7] \bullet H_2O$  and crystallizes in the monoclinic space group  $P2_1/c$ . The asymmetric unit contains four  $Cu(bpy)F(H_2O)_2^{2+}$  cations, two  $TaF_7^{2-}$  anions, and two unbound water molecules (Figure 3). Unlike the cations in compounds **1** and **2**, compound **3** is five coordinate and there are two of each  $\Delta$  and  $\Lambda$  enantiomer in the asymmetric unit. There are two sets of heterochiral  $\pi$ - $\pi$  stacking interactions: located at  $\sim \frac{1}{2}$  **c** and  $\sim \frac{1}{4}$  **c** and running along the **b** axis (Figure 3b). The resulting  $\pi$ - $\pi$  stacking interactions are of a head-to-tail orientation ( $T_1 = 131.904^\circ$ ) with both  $C_5N$  rings overlapping ( $T_2 = 97.766^\circ$ ) for interactions at  $\sim \frac{1}{2}$  **c**, while interactions at  $\sim \frac{1}{4}$  **c** are also head-to-tail oriented ( $T_1 = 100.111^\circ$ ) but with only one  $C_5N$  ring overlapping ( $T_2 = 51.043^\circ$ ). Further characterization of the cation included an evaluation with the  $\tau_5$  parameter. This parameter is a measure of the molecular geometry of a 5-coordinate metal center with the formula  $\tau_5 = \frac{\beta-\alpha}{60}$ , where  $\beta$  and  $\alpha$  are the two largest valence angles

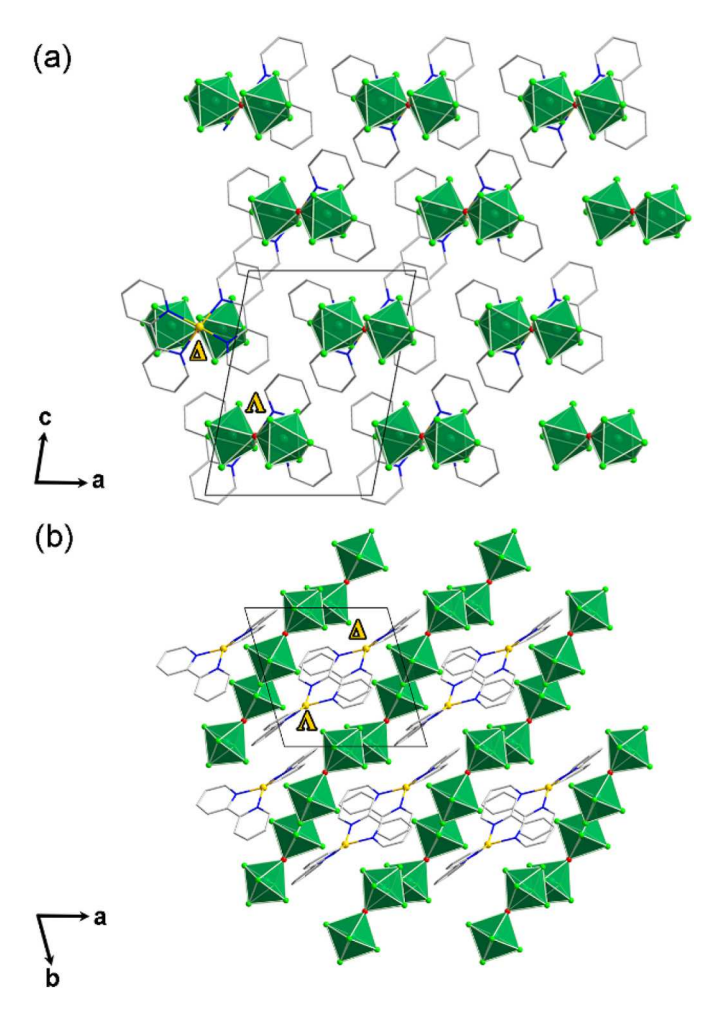


Fig. 2. Structure of Compound 2 as viewed down the (a)  $\mathbf{b}$  axis, and the (b)  $\mathbf{c}$  axis. Dark green, yellow, light green, red, blue, and gray spheres represent Ta, Cu, F, O, N, and C respectively, green polyhedra represent Ta-centered anions. Hydrogen atoms on the ligands have been omitted for clarity.

[43]. For compound 3,  $\tau_5$  ranges from 0.206 to 0.371, which are intermediate between a square pyramidal geometry ( $\tau_5 = 0$ ) and a trigonal bipyramidal geometry ( $\tau_5 = 1$ ).

Two  $TaF_7^{2-}$  anions are present in each asymmetric unit, both with pentagonal bipyramidal geometry. Neither pentagonal ring is planar and between the anions, the 14 Ta–F bond lengths vary from 1.900 to 2.010 Å, with the longest bond in each anion present in the pentagonal ring.

Compound 3 exhibits a hydrogen bonding network that interconnects the cations, anions, and free water molecules (Fig. 3c). On each anion, four of the five equatorial F atoms hydrogen bond with water molecules bound to the cation; one F interacts with both bound water molecules on a neighboring cation, two F interact with free water molecules.

# 3.2. Reduction of Cu in Compound 1

The crystals of compound 1 were observed as an orange/amber color, suggesting the reduction of the  $\text{Cu}^{2+}$  starting reagent to  $\text{Cu}^+$  in the products. This reduction was further confirmed by structural solution of compound 1, as the cation co-crystalizes with a known 1 anion (TaF $_6$ ), necessitating a cation charge of 1+ for charge balance.

While the precise mechanism of the reduction of Cu<sup>2+</sup> to Cu<sup>+</sup> cannot be elucidated with certainty, and the reducing agent unidentified, the authors speculate that the increased reaction temperature—and therefore pressure—from which compound 1 crystallized from contributed to an increased susceptibility of Cu<sup>2+</sup> reduction [44]. Reduction of Cu<sup>2+</sup>

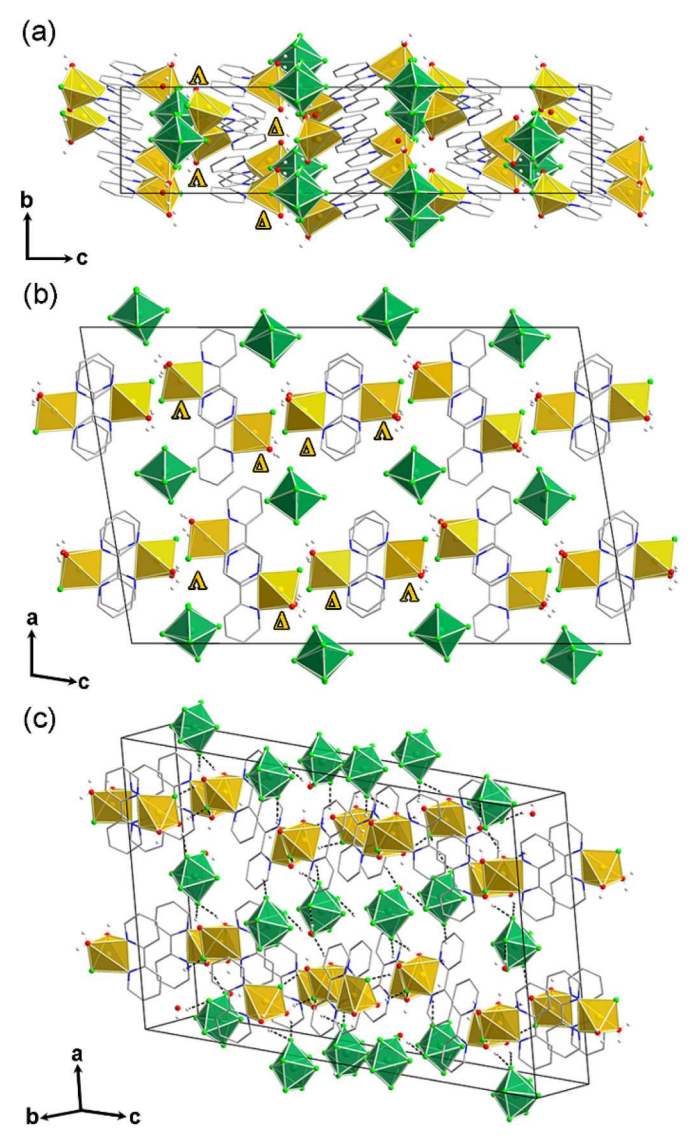


**Fig. 3.** Structure of Compound **3** as viewed down the (a) **a** axis, and the (b) **b** axis. Hydrogen bonding network between coordination water hydrogen and anions is shown in (c), H-bonds are depicted with dashed black lines. Dark green, yellow, light green, red, blue, and gray spheres represent Ta, Cu, F, O, N, and C, respectively, green polyhedra represent Ta-centered anions and yellow polyhedra represent Cu-centered cations. Non-coordinating water and hydrogen atoms on the ligands have been omitted for clarity.

was only observed at the elevated temperature of 200  $^{\circ}$ C and observed in all reactions conducted at this temperature, implying that the increase in temperature is a major driving force for the formation of Cu<sup>+</sup> ions. Further, the Cu<sup>+</sup> ions are stabilized in solution at 200  $^{\circ}$ C owing to the considerably decreased dielectric constant of water at this temperature, allowing the suppression of the Cu<sup>+</sup> disproportionation reaction [45].

# 3.3. Formation of Different Ta-Oxyfluoride Anions

Since the 1970s, the formation of different oxyfluoride anions has been studied in relation to the organic bases in solution—beginning with Olah's reagent as a nucleophilic fluorinating agent [18,19,46–50]. Within the realm of Ta-oxyfluoride anion formation in the presence of hydrofluoric acid, the  $pK_a$  of the organic bases allows for control over which anion species form: for instance, a high  $pK_a$  base such as quinuclidine ( $pK_a = 10.87$ ) grants a higher concentration of fluoride anions, while a smaller  $pK_a$  base—like 2,2′-bipyridine ( $pK_a = 4.23$ )—yields

lower fluoride concentrations [18,19]. Ligands with high  $pK_a$  value are more readily protonated by hydrofluoric acid in solution, leading to a higher dissociation of the acid into  $H^+$  and  $F^-$  ions. The opposite is also true, ligands with low  $pK_a$  values are protonated less and therefore do not lead to much HF dissociation. It was also observed that formation of oxyfluoride anions does not occur with organic ligands with  $pK_a$  values lower than that of the weak hydrofluoric acid ( $pK_a = 3.17$ ) [18].

In this study, only one organic base, 2,2'-bipyridine (bpy), was used across a large phase space with differing ratios of base to metal-oxides (Fig. 4, x axis) as well as through a range of pH values (Fig. 4, y axis) with the aim of creating compounds formed of discrete Ta-oxyfluoride anions and Cu-bpy cations. The case of making metal-ligand cations differs from the aforementioned studies in that the protonation of the ligand does not occur appreciably, and therefore the equilibrium established between ligand basicity and HF dissociation is less pronounced.

Without organic bases to protonate, what is the relationship between the concentration of the organic base in solution and the fluoride ion concentration and subsequently, the Ta-oxyfluoride anion formed? When the ratio of ligand to metal-oxide starting reagents (CuO and Ta<sub>2</sub>O<sub>5</sub>, which are held at a constant ration of 1 mol Cu:1 mol Ta) is low, only Ta-fluoride anions form and as the ratio increases beyond 2:1, Taoxyfluoride anions appear at low acid concentrations. The preference for formation of fluoride ions over oxyfluoride ions appears to be an issue of solubility; at low acid and base concentrations (low ratio, 1:1 and high pH), the tantalum oxide starting reagent is not completely soluble, consistent with previous findings [51-53]. Incomplete dissociation of Ta<sub>2</sub>O<sub>5</sub> creates a relatively higher [F<sup>-</sup>]:[Ta<sup>5+</sup>] ratio, leading to the formation of fluoride-rich anions. As the base:metal-oxide ratio increases, a trend can be perceived by moving from left to right in Fig. 4, Ta<sub>2</sub>O<sub>5</sub> becomes more soluble, leading to the anion formation rules previously established by Lu and Wu [18,19]. At low base:metal-oxide starting ratios, the pKa of the solution can be thought of as being lower—closer to that of hydrofluoric acid—but instead of decreasing the dissociation of HF, there is limited Ta<sub>2</sub>O<sub>5</sub>. It has been noted that early transition metal(ETM)-oxyfluoride anions have not been observed with ratios of base:ETM less than 1.5, hinting that this is an upper limit for ETM-oxide reaction and a lower limit for base-HF dissociation relationships.

When the organic base concentration in solution remains the same and the concentration hydrofluoric acid is added, the concentration of fluoride ions increases and the more fluoride rich anions form [28]. This trend can be viewed by taking any of the ligand:metal-oxide ratios found

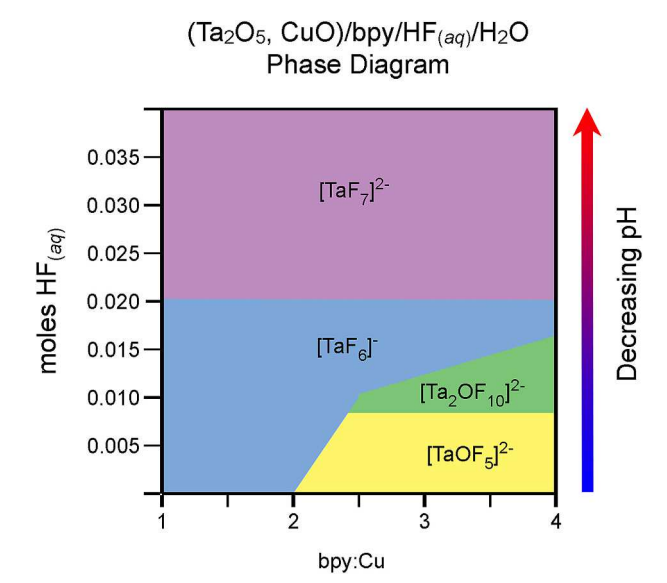


**Fig. 4.** Estimations of where different Ta–O/F anions can be found within the  $(Ta_2O_5,CuO)/bpy/HF_{(aq)}/H_2O$  phase diagram at 150 °C.

on the x-axis and moving upward. As the concentration of hydrofluoric acid is increased, the fluoride ion concentration increases to a level that eventually yields the fluoride only anions. A previous study showed that successively, the anions  $[TaOF_5]^{2^{-}}$ ,  $[TaF_6]^{-}$ ,  $[TaF_7]^{2^{-}}$ ,  $[TaF_8]^{3^{-}}$  and  $[TaF_9]^{4^{-}}$  form as concentration of acid is increased [28], additionally, the present work found that the intermediate anion  $[Ta_2OF_{10}]^{2^{-}}$  forms between the anions  $[TaOF_5]^{2^{-}}$  and  $[TaF_6]^{2^{-}}$ , in what appears be a narrow range. The fluoride rich anions  $[TaF_8]^{3^{-}}$  and  $[TaF_9]^{4^{-}}$  were not observed within the limits of acid concentrations used in this study.

Further, under the conditions tested in this study, the larger chain, prismatic, and tetrameric anions  ${\rm TaO_4F_4^{2-}}$ ,  ${\rm Ta_6O_9F_{18}^{6-}}$ , and  ${\rm Ta_4O_4F_{16}^{4-}}$ , respectively, were not observed, owing to the low  ${\rm p}K_{\rm a}$  of the bpy ligand and the limited range of acid concentrations used. It must also be noted that the boundaries depicted in Fig. 4 are largely estimated on the areas of phase space explored in this work and do not represent an exhaustive investigation of the phase space nor have they been rigidly defined experimentally.

## 4. Conclusions

Three new compounds were synthesized featuring three distinct Tafluoride or Ta-oxyfluoride anions. The phase space of (CuO,  $Ta_2O_5$ )/bpy/HF(aq)/H<sub>2</sub>O was investigated with differing ratios of ligand:metaloxide starting reagents as well as range of acid concentrations. It was found that fluoride-rich anions form in regions of high acid concentration and where metal-oxide starting reagents have limited reactivity; oxyfluoride anions form after a 1:1.5 threshold ratio of ligand:metaloxide and at low acid concentrations owing to limited dissociation of hydrofluoric acid. At any ligand:metal-oxide ratio, an increase in added acid concentration increases the amount of fluoride observed in the anion. These studies contribute to understanding new facets of mixed anion formation and allows for a targeted approach to designing materials with specific basic building units that can contribute to the emergence of physical properties.

# Associated content

Additional X-ray crystallographic data for compounds **1–3** (CCDC 2293940, 2293941, 2293943); additional structural characterization data for compound **1–3**.

#### CRediT authorship contribution statement

Kendall R. Kamp: Conceptualization, Investigation, Formal analysis, Writing – original draft, Writing – review & editing, Visualization. Yiran Wang: Conceptualization, Methodology, Writing – original draft. Kenneth R. Poeppelmeier: Supervision, Project administration, Funding acquisition.

#### Declaration of competing interest

The authors declare that they have no known competing financial interests or personal relationships that could have appeared to influence the work reported in this paper.

# Data availability

Data will be made available on request.

## Acknowledgment

This work was supported by fundings from the National Science Foundation (DMR-1904701) and the Joint Center for Energy Storage Research. Single crystal diffraction data and UV-Visible spectrometry was collected at the Integrated Molecular Structure Education and Research Center (IMSERC) at Northwestern University which has

received support from the Soft and Hybrid Nanotechnology Experimental (SHyNE) Resource (NSF ECCS-1542205), the State of Illinois, the International Institute for Nanotechnology (IIN), and the National Science Foundation (DMR-0521267). The authors thank Ms. C. Stern for experimental assistance with single crystal diffraction and Dr. C. Malliakas for help with UV-Visible spectroscopy measurements.

#### Appendix A. Supplementary data

Supplementary data to this article can be found online at https://doi.org/10.1016/j.solidstatesciences.2023.107369.

#### References

- [1] R. Gautier, K.R. Poeppelmeier, Alignment of Acentric units in infinite chains: a "Lock and Key" model, Cryst. Growth Des. 13 (9) (2013) 4084–4091.
- [2] P.S. Halasyamani, K.R. Poeppelmeier, Noncentrosymmetric oxides, Chem. Mater. 10 (10) (1998) 2753–2769.
- [3] W. Zhang, H. Yu, H. Wu, P.S. Halasyamani, Phase-matching in nonlinear optical compounds: a materials perspective, Chem. Mater. 29 (7) (2017) 2655–2668.
- [4] M.D. Donakowski, R. Gautier, J. Yeon, D.T. Moore, J.C. Nino, P.S. Halasyamani, K. R. Poeppelmeier, The role of polar, Lamdba (A)-Shaped building units in noncentrosymmetric inorganic structures, J. Am. Chem. Soc. 134 (18) (2012) 7679–7689.
- [5] O. Andersen, O. Jepsen, M. Sob, M. Yussouff, Electronic band structure and its applications, LNP 283 (1987) 1.
- [6] J. Singleton, Band Theory and Electronic Properties of Solids, vol. 2, OUP Oxford, 2001.
- [7] A. Ramirez, Geometrical frustration, Handb. Magn. Mater. 13 (2001) 423-520.
- [8] M.-s. Miao, J. Botana, E. Zurek, T. Hu, J. Liu, W. Yang, Electron counting and a large family of two-dimensional semiconductors, Chem. Mater. 28 (7) (2016) 1994–1999.
- [9] D. Zhang, H. Wu, C.R. Bowen, Y. Yang, Recent advances in pyroelectric materials and applications, Small 17 (51) (2021), 2103960.
- [10] W.P. Mason, H. Baerwald, Piezoelectric crystals and their applications to ultrasonics, Phys. Today 4 (5) (1951) 23–24.
- [11] I. Hagemann, Q. Huang, X. Gao, A. Ramirez, R. Cava, Geometric magnetic frustration in Ba<sub>2</sub>Sn<sub>2</sub>Ga<sub>3</sub>ZnCr<sub>7</sub>O<sub>22</sub>: a two-dimensional spinel based Kagomé lattice, Phys. Rev. Lett. 86 (5) (2001) 894.
- [12] H. Karunadasa, Q. Huang, B. Ueland, J. Lynn, P. Schiffer, K. Regan, R. Cava, Honeycombs of triangles and magnetic frustration in SrL<sub>2</sub>O<sub>4</sub> (L= Gd, Dy, Ho, Er, Tm, and Yb), Phys. Rev. B 71 (14) (2005), 144414.
- [13] H. Kageyama, K. Hayashi, K. Maeda, J.P. Attfield, Z. Hiroi, J.M. Rondinelli, K. R. Poeppelmeier, Expanding frontiers in materials chemistry and physics with multiple anions, Nat. Commun. 9 (1) (2018) 772.
- [14] R. Gautier, A.J. Norquist, K.R. Poeppelmeier, From racemic units to polar materials, Cryst. Growth Des. 12 (12) (2012) 6267–6271.
- [15] M.L. Nisbet, I.M. Pendleton, G.M. Nolis, K.J. Griffith, J. Schrier, J. Cabana, A. J. Norquist, K.R. Poeppelmeier, Machine-learning-assisted synthesis of polar racemates, J. Am. Chem. Soc. 142 (16) (2020) 7555–7566.
- [16] M. Kraft, J.R. Flores, W. Klopper, M.M. Kappes, D. Schooss, Structures of small tantalum cluster anions: experiment and theory, J. Phys. Chem. A 125 (15) (2021) 3135–3145.
- [17] S. Schreiner, L.E. Aleandri, D. Kang, J.A. Ibers, Solid-state chalcogenide anions of tantalum and niobium: synthesis and structures of the Ta<sub>2</sub>S<sub>11</sub><sup>4</sup> and Nb<sub>4</sub>Se<sub>22</sub><sup>6</sup> anions, Inorg. Chem. 28 (3) (1989) 392–393.
- [18] H. Lu, R. Gautier, M.D. Donakowski, L. Fuoco, Z. Liu, K.R. Poeppelmeier, Specific chemistry of the anions: [TaOF<sub>5</sub>]<sup>2</sup>-, [TaF<sub>6</sub>]<sup>-</sup>, and [TaF<sub>7</sub>]<sup>2</sup>-, Cryst. Growth Des. 14 (2) (2014) 844–850.
- [19] L.-K. Wu, Q.-Q. Hu, Z.-J. Wang, Z.-Q. Xie, Y. Feng, Q.-H. Zou, H.-Y. Ye, J.-R. Li, Controlling the assembly of tantalum oxyfluoride anions by organic amine cations: from molecular cluster, molecular cage to polymeric chain, Cryst. Growth Des. 23 (7) (2023) 5257–5263.
- [20] M.E. Welk, A.J. Norquist, F.P. Arnold, C.L. Stern, K.R. Poeppelmeier, Out-of-center distortions in d<sup>0</sup> transition metal oxide fluoride anions, Inorg. Chem. 41 (20) (2002) 5119–5125.
- [21] C. Lenoir, K. Boubekeur, P. Batail, E. Canadell, P. Auban, O. Traetteberg, D. Jérome, (TMTSF)<sub>3</sub>Ta<sub>2</sub>F<sub>11</sub>: synthesis, structural chemistry, electronic structure and physical properties, Synth. Met. 42 (1–2) (1991) 1939–1942.
- [22] A. Ruiz-Martínez, D. Casanova, S. Alvarez, Polyhedral structures with an Odd Number of vertices: Nine-coordinate metal compounds, Chem. Eur J. 14 (4) (2008) 1291–1303.
- [23] M.A. Saada, A. Hémon-Ribaud, M. Leblanc, V. Maisonneuve, Anion and cation disorder in [CN<sub>3</sub>H<sub>6</sub>]·(TaF<sub>6</sub>), Solid State Sci. 7 (9) (2005) 1070–1073.
- [24] M.A. Saada, A. Hémon-Ribaud, L.S. Smiri, M. Leblanc, V. Maisonneuve, Two tantalum fluorides templated with tren: [H<sub>4</sub>tren](TaF<sub>7</sub>)<sub>2</sub>·H<sub>2</sub>O and [H<sub>4</sub>tren](TaF<sub>7</sub>)<sub>2</sub>, J. Fluor. Chem. 126 (8) (2005) 1246–1251.
- [25] Y. Feng, Z. Meng, Q. Huang, D. Qiu, H. Shi, Hydrothermal syntheses, crystal structures and characterizations of two new metal-fluorides based on niobium and tantalum, Inorg. Chem. Commun. 13 (10) (2010) 1118–1121.
- [26] Y. Feng, L. Wang, Z. Xing, Q. Huang, P. Ma, A new Cu(II) coordination polymer constructed from two kinds of ligands and rare [Ta<sub>2</sub>OF<sub>10</sub>]<sup>2-</sup> anion: synthesis,

- crystal structure and fluorescent properties, Inorg. Chem. Commun. 93 (2018)
- [27] J. Sala-Pala, J.E. Guerchais, A.J. Edwards, [Ta<sub>4</sub>F<sub>12</sub>O<sub>6</sub>]<sup>4-</sup>: a Tetranuclear Fluorooxotantalate (V) with adamantane Skeleton, Angew. Chem., Ind. Ed. Engl. 21 (11) (1982) 870–871.
- [28] F. Monroy-Guzman, D. Truber, L. Brillard, M. Hussonnois, O. Constantinescu, C. L. Naour, Anion exchange behaviour of Zr, Hf, Nb, Ta and Pa as homologues of Rf and Db in fluoride medium, J. Mex. Chem. 54 (1) (2010) 24–33.
- [29] Y. Kasamatsu, A. Toyoshima, H. Haba, H. Toume, K. Tsukada, K. Akiyama, T. Yoshimura, Y. Nagame, Adsorption of Nb, Ta and Pa on anion-exchanger in HF and HF/HNO<sub>3</sub> solutions: Model experiments for the chemical study of Db, J. Radioanal. Nucl. Chem. 279 (2) (2009) 371–376.
- [30] T.M. Alam, J.S. Clawson, F. Bonhomme, S.G. Thoma, M.A. Rodriguez, S. Zheng, J. Autschbach, A solid-state NMR, X-ray diffraction, and Ab initio investigation into the structures of Novel tantalum oxyfluoride clusters, Chem. Mater. 20 (6) (2008) 2205–2217.
- [31] D. Peters, R. Miethchen, Symptoms and treatment of hydrogen fluoride injuries, J. Fluor. Chem. 79 (2) (1996) 161–165.
- [32] J.C. Bertolini, Hydrofluoric acid: a review of toxicity, J. Emerg. Med. 10 (2) (1992)
- [33] E.B. Segal, First aid for a unique acid, HF: a sequel, J. Chem. Health Saf. 7 (1) (2000) 18–23.
- [34] M.L. Nisbet, E. Hiralal, K.R. Poeppelmeier, Crystal structures of three copper(II)-2,2"-bipyridine (bpy) compounds, [Cu(bpy)<sub>2</sub>(H<sub>2</sub>O)][SiF<sub>6</sub>]\*4H<sub>2</sub>O, [Cu (bpy)<sub>2</sub>(TaF<sub>6</sub>)<sub>2</sub>] and [Cu(bpy)<sub>3</sub>][TaF<sub>6</sub>]<sub>2</sub> and a related coordination polymer, [Cu (bpy)(H<sub>2</sub>O)<sub>2</sub>SnF<sub>6</sub>]<sub>n</sub>, Acta Crystallogr. E. 77 (2) (2021) 158-164.
- [35] C. CrysAlisPRO, Oxford Diffraction/Agilent Technologies UK Ltd, 2011. Yarnton, England.
- [36] G. Sheldrick, SHELXTL: Software Suite for the Determination of Crystal Structures, Bruker Analytical X-ray Systems Inc., Madison, Wisconsin, United States, 2000, Version 6.12.
- [37] O.V. Dolomanov, L.J. Bourhis, R.J. Gildea, J.A. Howard, H. Puschmann, OLEX<sup>2</sup>: a complete structure solution, refinement and analysis program, J. Appl. Crystallogr. 42 (2) (2009) 339–341.
- [38] L. Yang, D.R. Powell, R.P. Houser, Structural variation in copper(i) complexes with pyridylmethylamide ligands: structural analysis with a new four-coordinate geometry index, τ<sub>4</sub>, Dalton Trans. (9) (2007) 955–964.
- [39] P.V. Petrović, G.V. Janjić, S.D. Zarić, Stacking interactions between square-planar metal complexes with 2,2'-bipyridine ligands. Analysis of crystal structures and Ouantum chemical Calculations, Cryst. Growth Des. 14 (8) (2014) 3880–3889.
- [40] Y. Wang, M.L. Nisbet, K.R. Kamp, E. Hiralal, R. Gautier, P.S. Halasyamani, K. R. Poeppelmeier, Beyond π–π stacking: understanding inversion symmetry

- breaking in crystalline racemates, J. Am. Chem. Soc. 145 (30) (2023) 16879–16888
- [41] J.C. Dewan, A.J. Edwards, J.Y. Calves, J.E. Guerchais, Fluoride crystal structures. Part 28. Bis(tetraethylammonium)μ-oxo-bis[pentafluorotantalate(V)], J. Chem. Soc. Dalton Trans. (10) (1977) 978–980.
- [42] Z.-H. Meng, Y.-Q. Feng, X.-F. Chen, 5, 6-Dihydro-1, 10-phenanthroline-1, 10-diium μ-oxido-bis [pentafluoridotantalate (V)], Acta Crystallogr. E. 68 (5) (2012) m561, m561.
- [43] A.W. Addison, T.N. Rao, J. Reedijk, J. van Rijn, G.C. Verschoor, Synthesis, structure, and spectroscopic properties of copper(II) compounds containing nitrogen-sulphur donor ligands; the crystal and molecular structure of aqua[1,7-bis(N-methylbenzimidazol-2/-yl)-2,6-dithiaheptane]copper(II) perchlorate, J. Chem. Soc. Dalton Trans. 7 (1984) 1349–1356.
- [44] N.N. Greenwood, A. Earnshaw, Chemistry of the Elements, Elsevier, 2012.
- [45] G.C. Akerlof, H.I. Oshry, The dielectric constant of water at high temperatures and in equilibrium with its vapor, J. Am. Chem. Soc. 72 (7) (1950) 2844–2847.
- [46] H. Lu, R. Gautier, M.D. Donakowski, Z. Liu, K.R. Poeppelmeier, From solution to the solid state: control of niobium oxide-fluoride [NbO<sub>x</sub>F<sub>y</sub>]<sup>n-</sup> species, Inorg. Chem. 53 (1) (2014) 537–542.
- [47] G. Olah, J. Shih, G. Prakash, Fluorine-containing reagents in organic synthesis, J. Fluor. Chem. 33 (1-4) (1986) 377-396.
- [48] G.A. Olah, J.T. Welch, Y.D. Vankar, M. Nojima, I. Kerekes, J.A. Olah, Synthetic methods and reactions. 63. Pyridinium poly(hydrogen fluoride) (30% pyridine-70% hydrogen fluoride): a convenient reagent for organic fluorination reactions, J. Org. Chem. 44 (22) (1979) 3872–3881.
- [49] P. Halasyamani, M.J. Willis, C.L. Stern, K.R. Poeppelmeier, Crystal growth in aqueous hydrofluoric acid and (HF)<sub>x</sub>· pyridine solutions: syntheses and crystal structures of [Ni(H<sub>2</sub>O)<sub>6</sub>]<sup>2+</sup>[MF<sub>6</sub>]<sup>2-</sup>(M= Ti, Zr, Hf) and Ni<sub>3</sub>(py)<sub>12</sub>F<sub>6</sub>·7H<sub>2</sub>O, Inorg. Chim. Acta. 240 (1–2) (1995) 109–115.
- [50] K.R. Heier, A.J. Norquist, C.G. Wilson, C.L. Stern, K.R. Poeppelmeier, [pyH]<sub>2</sub>[Cu (py)<sub>4</sub>(MX<sub>6</sub>)<sub>2</sub>] (MX<sub>6</sub> = ZrF<sub>6</sub><sup>2</sup>, NbOF<sub>5</sub><sup>2</sup>, MoO<sub>2</sub>F<sub>4</sub><sup>2</sup>; py = pyridine): rarely observed Ordering of metal oxide fluoride anions, Inorg. Chem. 37 (1) (1998) 76–80.
- [51] P.S. Halasymani, K.R. Heier, A.J. Norquist, C.L. Stern, K.R. Poeppelmeier, Composition space of the (CdO, 0.5Nb<sub>2</sub>O<sub>5</sub>)/(HF)<sub>x</sub>-Pyridine/H2O system. Structure and synthesis of CdNb(py)<sub>4</sub>OF<sub>5</sub>, Inorg. Chem. 37 (2) (1998) 369–371.
- [52] A.J. Norquist, K.R. Heier, C.L. Stern, K.R. Poeppelmeier, Composition space diagrams for mixed transition metal oxide fluorides, Inorg. Chem. 37 (25) (1998) 6495–6501.
- [53] A.J. Norquist, C.L. Stern, K.R. Poeppelmeier, Cu(C<sub>10</sub>H<sub>9</sub>N<sub>3</sub>)<sub>2</sub>MOF<sub>5</sub>: 2H<sub>2</sub>O (M = Nb, Ta): Aligned [MOF<sub>5</sub>]<sup>2</sup>· oxide fluoride anions, Inorg. Chem. 38 (15) (1999) 3448–3449.